REVIEWS OF GEOPHYSICS, SUPPLEMENT, PAGES 132-137, APRIL 1991
U.S. NATIONAL REPORT TO INTERNATIONAL UNION OF GEODESY AND GEOPHYSICS 1987-1990

Geophysical Applications of Satellite Altimetry

DAVID T. SANDWELL

Geological Research Division, Scripps Institution of Oceanography, La Jolla, CA 92093

INTRODUCTION

The most significant development in the field of "geophysical applications of satellite altimetry" over the last 4 years has been the Geosat altimeter mission. While the Geos-3 and Seasat missions [see Geos-3 Special Issue, 1979; Seasat Special Issue I, 1982; Seasat Special Issue II, 1983] demonstrated the potential of satellite altimetry for the recovery of the marine geoid and gravity field, Geosat has nearly realized the full potential of this method. Papers published over the past 4 years confirm the importance of these data for many geological and geophysical applications. Moreover, the high accuracy and resolution achieved by the Geosat altimeter suggests that data collected (or declassified) over the next decade will provide our first global view of the ocean basins at a resolution of 10 km. For the reader interested in an overview of the satellite altimeter method as well as basic orbit mechanics see chapters 14 and 15 of Stewart [1985].

The U.S. Navy satellite Geosat was launched on March 12, 1985 into an 800 km altitude, nearly circular orbit with an inclination of 108° [Jensen and Wooldridge, 1987; McConathy and Kilgus, 1987]. During the first 18 months of the primary Geosat Geodetic Mission (Geosat/GM), the orbit of the spacecraft was allowed to drift so that ground tracks did not repeat on a regular basis. This resulted in 200 million kilometers of sea surface topography profile having an average ground track spacing of 4 km over all ocean areas between 72°N and 72°S. Most of these data are classified although data south of 60°S in Antarctic waters were recently declassified and reveal the full potential of the high-density coverage (Figure 1) [McAdoo et al., 1990]. Papers discussing the Geosat radar altimeter [MacArthur et al., 1987], its performance [Sailor and LeSchack, 1987], and determination of the ocean geoid [Smith III et al., 1987; Van Hee, 1987] are found in a special issue of *Johns Hopkins APL Technical Digest* [vol. 8, no. 2, 1987] devoted to the Navy Geosat Mission.

After completion of the nominal 18-month geodetic mission, the spacecraft was placed into a 17-day exact repeat orbit suitable for observing changes in sea surface topography associated with mesoscale ocean currents. The orbit was arranged to follow the Seasat ground track to within 11 km and repeat within a 1 km swath along a 17-day repeat track [Born et al., 1987]. This repeat orbit was maintained for 68 cycles (3-years) until the tape recorders on the spacecraft finally failed after almost 5 years of continuous operation! These data can be obtained from the National Ocean Data Center [Cheney et al., 1987].

Since the data from the Geosat Exact Repeat Mission (Geosat/ERM) were not classified, and the ERM track was chosen for observing ocean dynamics [Mitchell et al., 1987], most of the published literature on Geosat altimetry is related to physical oceanography. These oceanographic applications require much greater accuracy than is needed for the recovery of the marine geoid and especially the marine gravity field [Stewart, 1985]. A special issue of Journal of Geophysical Research - Oceans [vol. 95, no. C3, 1990] is devoted to unclassified research using Geosat altimetry [Douglas and Cheney, 1990]. In addition to these special journal issues on Geosat, there are many publications related to geophysical applications of Seasat and Geosat altimetry. The remainder of this report divides these applications into 5 sections; Geoid and Gravity Errors, Regional Geoid Heights and Gravity Anomalies, Local Gravity Field/Flexure, Plate Tectonics and Gridded Geoid Heights/Gravity Anomalies.

GEOID AND GRAVITY ERRORS

Errors in sea surface topography measurements arise from altitude measurement errors, and radial orbit errors. For geophysical applications, one is interested in geoid height so that ocean dynamic topography and tides are also considered as error sources. At the global scale (4000 - 40000 km), the most accurate geoid height models are derived by tracking and modelling the orbits of many artificial satellites. Satellite altimeter data have also been incorporated into these global solutions and various methods have been used to decompose the sea surface topography into the marine geoid and the dynamic topography [Tapley et al., 1988; Marsh et al., 1990; Denker and Rapp, 1990]. While the geoid height is known quite accurately at the global scale, most recent geophysical applications of satellite altimetry tend to be regional (400 - 4000 km) and local scale (< 400 km) studies where the absolute height of the sea surface above the reference ellipsoid is rarely an important consideration; instead changes in *geoid height* within the region are desired. In many studies, especially at the local scale, the geoid height measurements are converted to gravity anomalies or deflections of the vertical (i.e. geoid slope). Since these quantities are both spatial derivatives of the gravitational potential (or geoid height), errors in sea surface slope are the most important consideration. One microradian (μrad) of sea surface slope corresponds to 0.98 milligal (mgal) of along-track gravity disturbance. The sources and magnitude of error in sea surface slope are given in the Table 1.

Paper number 91RG00539
8755-1209/91/91RG00539 $15.00

TABLE 1. Errors in Sea Surface Slope

Error Source	Height (m)	Length Scale (km)	Slope (μrad)
Land, Ice	< 4.0	10	< 400
Dynamic Topography	1.0	> 100	< 10
Altimeter Noise	0.05	> 10	<5
Wet Troposphere	< 0.1	> 100	< 1.0
E/M Bias	0.1	> 200	< 0.5
Height Acceleration	< 0.02	> 70	< 0.5
Orbit GDR	3.0	10000	0.30
Ocean Tide	0.10	> 1000	< 0.10
Ionosphere	0.10	> 1000	< 0.10
Orbit GEM-T1	0.85	10000	0.085

The largest slope errors occur when the altimeter footprint intersects land or ice causing a a rapid change in elevation that is unrelated to the geoid [Brooks and Lockwood, 1990]. For example, at a coastline a 4 meter change in elevation can occur over a distance of a few Geosat footprints (~ 10 km) resulting in a slope error of 400 μrad. The land radar reflections can be eliminated with a very precise land-sea mask, however, early radar returns from sea ice can only be edited by comparing the data with previous or nearby measurements. The second largest source of sea surface slope error (< 10 μrad) is caused by changes in elevation associated with western boundary currents (i.e. dynamic topography) [Zlotnicki and Marsh, 1989]. This dynamic topography has a scale ranging from 100 km to 10,000 km and can de divided into a permanent component and a component that varies with time.

Altimeter noise, which is primarily due to inaccurate determinations in the round-trip travel time of the radar pulse, is a major source of error especially at short wavelengths [Marks and Sailor, 1986; LeSchack and Sailor, 1988]. Individual Geosat altimeter profiles have an rms slope error of about 6 μrad although this can be reduced to less than 1 μrad by averaging many repeat profiles [Sandwell and McAdoo, 1990]. The averaging also increases the along-track resolution of the Geosat data from about 30 km (full wavelength) to about 20 km. However, because "repeating" profiles repeat only within a 1 km band, one must be especially careful when averaging or differencing repeat profiles in areas where the sea surface slope is high [Brenner et al., 1990].

The remaining error sources make almost negligible contributions to the slope error budget either because the height errors are less than 0.1 m or because these errors have a large correlation length. Errors in the wet tropospheric correction [Zimbelman and Busalacchi, 1990; Monaldo, 1990; Emery et al., 1990; Liu and Mock, 1990] are generally less than 0.1 meter and occur over a length scale of greater than 100 km resulting in a slope error of less than 1 μrad. Similarly, the electromagnetic bias caused by stronger radar return from a wave trough than a wave crest, is generally less than 0.1 m and has a length scale of greater than 200 km resulting in a slope error of less than 0.5 μrad [Hayne and Hancock, 1990; Walsh and Jackson, 1989; Ping, 1990]. The height acceleration, or curvature in the altitude profile, can also introduce slope measurement errors which are generally less than about 0.5 μrad (< 0.02 m over a length > 70 km) [Hancock et al., 1990].

Radial orbit error, which is major error source for oceanographic applications, is only a minor contribution to the slope error budget. For example, the operational orbit error distributed with the Geosat/ERM geophysical data records [Cheney et al., 1987] is known to have errors of 3 m rms and a correlation length of greater than 10000 km; this results in a slope error of less than 0.3 μrad. Using more tracking data and improved gravity models (e.g. GEM T-1), the radial orbit error in Geosat altimeter profiles has been reduced to 0.85 m [Shum et al., 1990; Haines et al., 1990]. This reduces the slope error to < 0.085 μrad. Errors in the ocean tide models can range up to 0.1 m and generally have a length scale of greater than 1000 km [Cartwright and Ray, 1990] resulting in a slope error of less than 0.1 μrad. Finally unmodelled delays of the radar pulse, as it propagates through the ionosphere, can produce a height error which is generally less than 0.1 m over a length scale of generally greater than 1000 km [Musman et al., 1990] resulting in a slope error of less than 0.1 μrad.

In summary, the major sources of error in the regional geoid height, gravity anomalies and vertical deflections are land/ice radar returns, short-wavelength dynamic topography, and broad-band altimeter noise. Repeating altimeter profiles can be used to identify errant radar returns from land and ice and thus eliminate these errors. Moreover, averaging many repeats can reduce the errors in sea surface due to both changes in dynamic topography and altimeter noise as long as these errors are uncorrelated in time. Errors due to unknown permanent dynamic topography cannot be reduced and therefore one must be careful when interpreting satellite altimeter profiles near areas if intense western boundary currents.

REGIONAL GEOID HEIGHTS AND GRAVITY ANOMALIES

During the past 4 years, several global geoid height and gravity anomaly models have been developed from satellite altimeter profiles [Marsh et al., 1986; Haxby, 1987; Pavlis and Rapp, 1990; W. F. Haxby personal communication; 1990]. Because of the nature of the satellite altimeter error budget, these models are quite accurate at the regional scale and thus have been used for investigations of lithospheric cooling with age [Jung and Rabinowitz, 1989] as well as the compensation depths of thermal swells and oceanic plateaus.

Several studies have compared the relationship between geoid height and topography on a global basis or over a large number of features. Rapp [1989] performed a global cross correlation between gravitational potential and topography. The goals of his study were: to determine the decrease in power with increasing spherical harmonic degree (5-180) for both geoid height and equivalent rock topography, to determine the correlation coefficient between the two spectra and to determine an average compensation depth assuming an Airy model (~30 km). Cazenave and Dominh [1987] examined the marine geoid/topography transfer function in the 1000 - 4000 km wavelength band in order to determine the average depth and mode of compensation; prior to the analysis they removed the effects of lithospheric cooling. Geoid/topography correlations exceeded 0.5 between wavelengths of 1000 and 2000 km and the average ratio was 2.5 m/km.

Other studies isolated individual oceanic swells and plateaus prior to calculating the geoid/topography ratios. There is still some debate on how the longest wavelength components of the geoid should be removed. Sandwell and Renkin [1988] calculated geoid/topography ratios over 10 swells and plateaus in the North Pacific and found the highest

ratio associated with the southeast end of the Hawaiian Swell (5.5 m/km) and lower ratios further downstream from the hotspot. The lowest ratios (1 - 2 m/km) were observed over Airy-compensated plateaus. A similar global study of 53 areas [Sandwell and MacKenzie, 1989] was also performed to establish the compensation mechanisms of these features, especially the oceanic plateaus. Cazenave et al., [1988] performed a global analysis of 20 swells and troughs and discovered that the ratio of geoid height to topography increases as the square root of the age of the plate; a later study of 23 swells tends to confirm this result [Monnereau and Cazenave, 1990]. They interpreted this relationship as either due to increasing asthenospheric viscosity with lithospheric age or in terms of the increase in the thickness of the lithosphere at the expense of a constant viscosity asthenosphere.

The above analyses of geoid height versus topography over swells and plateaus were primarily concerned with a single admittance estimate over the intermediate wavelength band (400 - 4000 km). Because of this, it was impossible to separate the effect of crustal thickening from the deeper thermal compensation. A number of studies treated individual areas in greater detail in order to learn more about the strength and structure of the plate at the time the feature formed. An admittance approach was used to investigate the compensation mechanisms and flexural rigidity beneath the Del Cano Rise and Crozet Bank [Goslin and Diament, 1987], and the Mozambique Ridge [Maia et al., 1990]. Even using this standard admittance approach it is often difficult to differentiate among various compensation mechanisms. Because of this, a linear filter approach [McNutt and Shure, 1987] was used to investigate the compensation of the the Canary Island Group [Filmer and McNutt, 1989] and the Bermuda Rise [Sheehan and McNutt, 1989]. This same linear filter method was combined with heat flow observations to demonstrate that the Cape Verde Rise must be at least partially supported dynamically by a mantle plume [McNutt, 1988]. Geoid height and topography data were used with surface wave observations to suggest that the Superswell region of the south Pacific is dynamically supported by a broad mantle upwelling; the ratio of geoid height to topography is negative which is consistent with a low viscosity layer beneath the lithosphere [McNutt and Judge, 1990].

A number of studies focussed on the lineated gravity anomalies first discovered by Haxby and Weissel [1986] in the Pacific and Indian Oceans. While the original observations have been confirmed, there is still considerable debate concerning the origin of these features. Cazenave et al. [1987] performed a spectral analysis of the gravity lineations in the Indian Ocean and determined that they are oriented at N40°E, they have a characteristic wavelength of 200 km and they occur only on the northeast side of the southeast Indian Ridge. They speculated that the gravity lineations are due to small-scale convection that is organized into longitudinal rolls by the rapid absolute motion of the Indo-Australian plate. Moriceau and Fleitout [1989] performed a spectral analysis of the short-wavelength gravity lineations in 7 areas of the Pacific in order to compare their directions to present and past absolute plate motion directions. To reduce the edge effects associated with spectral analysis, they first constructed the Laplacian of the geoid (i.e. vertical gravity gradient). The directions of the gravity lineations in 6 of the 7 areas agreed fairly well with past and present absolute plate motion direction suggesting that the gravity lineations are related to either plume-like or roll-like convective motions in the mantle; the older lineations may be crustal expressions of earlier volcanic activity above numerous mantle plumes. Based on the discovery of en-echelon volcanos superimposed upon on of the more prominent gravity lineations, Winterer and Sandwell [1987] have suggested that the gravity lineations are lithospheric boudins caused by north-south extension of the Pacific plate. McAdoo and Sandwell [1989] analyzed the ratio of vertical deflections derived from repeat profiles of Geosat altimetry and 6 seafloor bathymetry profiles in the Central Pacific. They found no evidence of deep compensation for the gravity rolls suggesting that they are not dynamically supported. However, their results are quite uncertain because the coherence between gravity and seafloor topography is very low in the 200 km-wavelength band. Similar lineated gravity anomalies were discovered in the South Atlantic [Fleitout et al., 1989] and attributed to numerous plumes. More research is required to establish the origof these elusive features.

LOCAL GRAVITY/FLEXURE

Improvements in satellite altimeter measurements have enabled investigators to analyze the geoid signatures of relatively small scale features such as fracture zones, seamounts and spreading ridges. Geoid signatures across fracture zones (i.e. age offsets in the seafloor produced at transform faults) consist of a geoid step (reflecting a change in depth and thermal structure) [Crough, 1979] and flexural features within 200 km of the fracture zone. The lithospheric flexures are due to differential subsidence [Sandwell, 1984] and/or thermal bending moment [Parmentier and Haxby, 1986]. These multi-component models have been refined by Wessel and Haxby [1989; 1990] and now provide excellent fits to the new Geosat profiles in the Pacific. These recent models suggest that all three components (thermal edge effect, thermal bending moment and differential subsidence) are important along large-offset fracture zones (> 10 Ma offset). Moreover, Wessel and Haxby [1989] confirmed that measurements of the geoid step due to thermal subsidence will be systematically underestimated by 30-40% if the flexural effects are not considered. Sandwell [1984] found that the underestimate of the thermal step increases with fracture zone age from 20% at 20 Ma to 50% at 80 Ma if only flexure due to differential subsidence is considered. By properly accounting for the flexural effects, Wessel and Haxby [1989] found that lithospheric models, derived from depth versus age studies, are compatible with the geoid data across fracture zones. Several other studies did not account for the biases due to the flexural effects and found that the geoid steps across fracture zones were incompatible with the lithospheric cooling models [Gilbert et al., 1987; Marty and Cazenave, 1988; Driscoll and Parsons, 1988; Freedman and Parsons, 1990; Marty et al., 1988]; these studies required substantially thinner asymptotic plate thicknesses or plate thicknesses that varied with age. Small-scale convection was invoked to explain this anomalous behavior. Whether lithospheric flexure or small-scale convection is responsible for the reduction in measured geoid step amplitude, it has become clear that measurements of geoid steps do not provide robust estimates of the asymptotic thickness of the cooling lithosphere.

One of the major successes of satellite altimetry has been the mapping and characterization of seamounts. For example,

prior to the Seasat altimeter mission, the existing bathymetric soundings of the seamounts along the Lousiville Ridge were sparse. Seasat profiles revealed many uncharted volcanos along the Lousiville Ridge. These data were used to conduct a highly successful SeaBeam survey along the crest of the Lousiville hot spot chain [Lonsdale, 1988]. In addition, numerous Seasat profiles crossing the Louisville Ridge were used along with existing bathymetry and gravity data to estimate the flexural rigidity of the lithosphere when the seamounts formed [Watts et al., 1988]. Another shipboard study of the Austral archipelago has demonstrated that when a seamount is detected on at least two neighboring profiles the seamount can be located to a precision of 15 km [Baudry et al., 1987]. Craig and Sandwell [1988] examined all of the Seasat profiles to identify seamount signatures and to measure the peak to trough amplitudes of the features. Using 14 well surveyed seamounts in the Pacific, they found that the characteristic diameter of the seamount was equal to the distance between the peak and the trough in the vertical deflection profile. Seamount population densities were shown to vary substantially across major fracture zones; in the Pacific, the seamount population density decreases from the young side to the old side of the fracture zones. The major limitation in characterizing seamounts using Seasat and Geosat data is the large cross-track spacing between profiles.

In addition to locating seamounts, the amplitudes and widths of the gravity signatures can be used to estimate the effective elastic thickness of the lithosphere in areas where topography data are also available [Watts, 1979]. Studies of seamounts in the north Pacific showed that the effective elastic thickness is proportional to the square root of the age of the lithosphere when the seamount formed; the base of the elastic layer is approximately defined by the 450°C isotherm. New results from the Seasat data have shown that there is a broad area in the south-central Pacific where the elastic layer is thinner than expected [Calmant and Cazenave, 1987; Calmant et al., 1990]. Based on this evidence and other anomalies in the region, it was proposed that the lithosphere was thermally disrupted.

Vertical deflection profiles with very high accuracies (< 1 μrad or < 1 mgal) and resolutions (~ 20 km wavelength) have been constructed by averaging many repeat cycles of Geosat/ERM data [Sandwell and McAdoo, 1990]. This new globally uniform data set of along-track gravity profiles was used to examine spreading ridge axes on a global basis [Small and Sandwell; 1989]. Slow spreading ridges (< 60 mm/yr) usually have high amplitude gravity troughs (40-100 mgal), while fast spreading ridges (> 70 mm/yr) are characterized by low-amplitude ridge axis highs (~ 15 mgal). Unexpectedly, it was found that the transition from axial trough to axial high occurs abruptly at a spreading rate of 60-70 mm/yr. This result has provided important new constraints on physical models of spreading ridge axes.

PLATE TECTONICS

When it was discovered that oceanic fracture zones and transform faults produce prominent linear geoid anomalies that are apparent in satellite altimeter profiles [Haxby, 1987; Gahagan et al., 1988], it was evident that these data could be combined with magnetic anomaly profiles and shipboard bathymetry profiles to improve plate reconstructions of the oceans. To establish the relationship between the geoid signature of a fracture zone in relation to the fossil plate boundary, Shaw [1988] performed a detailed investigation of 1500 Seasat profiles crossing 15 small offset fracture zones in the south Atlantic. The the trough along each satellite altimeter profile roughly coincides with axis of the fracture zone. Moreover, it was shown that the depth of the geoid trough is inversely proportional to the spreading rate at the time of formation. Geoid and gravity troughs are also apparent along active transform faults and have been used along with bathymetric profiles, and earthquake slip vectors to determine 121 transform azimuths. These directional data were combined with 277 spreading rate estimated to construct a "current plate motion" model [DeMets et al., 1990]. A new feature in this plate model is a diffuse plate boundary located in the central Indian Ocean [Stein et al., 1989].

For detailed plate reconstructions, fracture zone lineations derived from satellite altimeter profiles, provide tight constraints on paleo-spreading directions. In addition, magnetic anomaly identifications, provide substantial information on the age of the seafloor as well as spreading rates but they are usually not sufficiently dense for accurate determination of spreading directions. Thus, most of the recent plate reconstruction models have combined these complementary data types. Seasat data have provided important new constraints on the opening of the South Atlantic [Shaw, 1987; Gilbert et al., 1989; Shaw and Cande, 1990] because shipboard coverage of this area is sparse. Seasat data [Stock and Molnar, 1987] and Geosat data [Mayes et al., 1990] were also combined with sparse shipboard coverage to greatly improve the plate reconstructions for the South Pacific for the late Cretaceous and Cenozoic periods. In the Indian ocean, Seasat data were combined with Mesozoic anomaly identifications and seismic reflection data to constrain the relative motion between Madagascar and Africa [Coffin and Rabinowitz, 1987; Cochran, 1988]. The Southwest Indian ridge [Royer et al., 1988] and Southeast Indian ridge [Royer and Sandwell, 1989] were reconstructed from the Late Cretaceous to the present time using new fracture zone constraints from Seasat and Geosat profiles. These Indian Ocean results are summarized in Royer et al. [1989]. Much recent work has focussed on Southern Ocean tectonics where shipboard data are sometimes very sparse. A reconstruction of the South American-Antarctic plate motion over the past 50 Ma has revealed a major change in spreading direction at 20 Ma [Barker and Lawver, 1988]. Because many repeat cycles of Geosat data span several Antarctic summers, coverage of the Southern Ocean gravity field is nearly complete up to the Antarctic coastline [Sandwell and McAdoo, 1988].

GRIDDED GEOID HEIGHTS/GRAVITY ANOMALIES

The major limitation of the existing (unclassified) satellite altimeter data sets is that the along-track resolution of the data is much better than the characteristic spacings of the altimeter profiles (Table 2) except in the area between 60°S and 72°S where the high-density Geosat Geodetic Mission data were recently declassified (Figure 1). Because of the poor coverage in the remaining ocean areas, some resolution is lost when the geoid profiles are interpolated onto a uniform grid. To partially overcome this problem, Haxby [1987] has identified lineations in the Seasat altimeter profiles; when a lineation crosses an area where there are no satellite observations, data

TABLE 2. Resolution of Gravity Field from Satellite Altimeter Profiles

Satellite	Precision (1 mgal = 0.98 μrad)	Along-Track Resolution, λ	Cross-Track[a] Resolution, λ
Geos-3	30 μrad	70 km[b]	20-400 km
Seasat	10 μrad	50 km[b]	~ 80 km
Geosat/ERM	< 1 μrad	20 km[c]	164 km
ERS-1[d]	< 1 μrad	20 km	82 km
Topex/Poseidon[d]	< 1 μrad	< 20 km	314 km

[a] Cross-track wavelength resolution is twice the characteristic track spacing at the equator.

[b] Along track wavelength resolution based on 0.5 coherence [Marks and Sailor, 1986].

[c] Along track wavelength resolution based on 0.5 coherence [Sandwell and McAdoo, 1990].

[d] Estimated accuracy and along-track resolution. Cross-track resolution based on planned orbit repeat cycle.

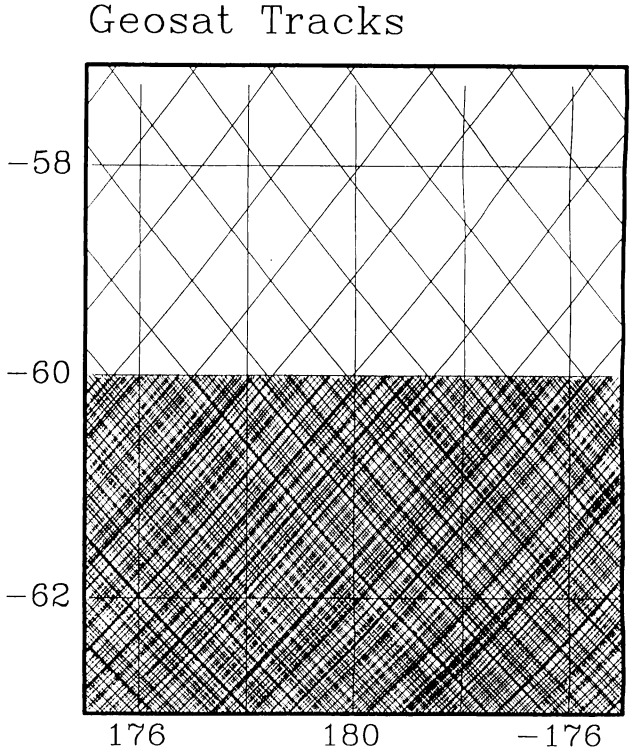

Fig. 1. Satellite altimeter profiles from the Geosat Geodetic Mission have a characteristic spacing of 2 km for latitudes between 60°S and 72°S. Satellite altimeter profiles from the Geosat Exact Repeat Mission (17-day repeat cycle) have much greater spacing (160 km at equator) but are not classified. In addition, many repeat cycles can be average to improve the along track accuracy and resolution.

points are added to guide the interpolation algorithm. This procedure greatly improves the resultant geoid or gravity anomaly surface but can also introduce false trends. In areas of dense Geos-3 coverage, Sandwell [1987] developed a 2-D biharmonic spline method that down-weights the Geos-3 data relative to the more accurate Seasat data. McAdoo [1990] has provided a summary of how gravity anomalies are constructed by first taking the along-track derivatives of the geoid height profiles. This differentiation avoids the crossover analysis problem which becomes increasingly difficult as spacings the satellite profiles decreases to less than the along-track resoltion of the data (< 10 km). Others have been quite successful at gridding Geosat profiles as well as combinations of Geos-3, Seasat and Geosat profiles [Hwang, 1989].

Bostrom [1989] has shown that the gridded gravity anomaly map produced by Haxby [1987] is quite valuable in discovering the presence of thick sediment accumulations. These data are used quite extensively by the petroleum exploration industry although most of the results are unpublished [see brochures by: Hayling, 1990; Fairhead, 1988]. Better coverage is required in almost all fields of marine geophysics but especially in the exploration community. The European Space Agency satellite ERS-1 will greatly improve the coverage of the marine geoid and gravity field especially when these data are combined with Geosat/ERM data and Seasat data. The Topex/Poseidon will also provide limited new coverage. However, to achieve the highest accuracy and resolution, a new dedicated satellite altimeter is required; the orbit of this new altimeter should not repeat on a time scale of less than 6 months in order to obtain cross-track resolution that is commensurate with the demonstrated along-track resolution. To obtain sub-milligal accuracy, the mission should last for about 5 years. This long lifetime can be used to reduce the random altimeter noise as well as the variations in sea surface topography due to ocean currents. Very recent results from declassified Geosat/GM data south of 60°S clearly demonstrate that improved altimeter coverage of the oceans will reveal all crustal features having dimensions greater than about 10 km. Such resolutions will not be achieved on a global basis by shipboard surveys in our lifetimes.

Acknowledgment. This work was supported by the National Aeronautics and Space Administration under grant NAG5-1226 and Scripps Institution of Oceanography.

REFERENCES

Barker, P. F., and L. A. Lawver, South American-Antarctic plate motion over the past 50 myr, and the evolution of the South American-Antarctic ridge, *Geophys. J.*, *94*, 377-386, 1988.

Baudry, N., M. Diament, and Y. Albouy, Precise location of unsurveyed seamounts in the Austral archipelago area using Seasat data, *Geophys. J. R. Astr. Soc.*, *89*, 869-888, 1987.

Born, G. H., J. L. Mitchell, and G. A. Heyler, Design of the Geosat exact repeat mission, *Johns Hopkins APL Technical Digest*, *8*, 260-266, 1987.

Bostrom, R. C., Subsurface exploration via satellite - structure visible in Seasat images of North Sea, Atlantic Continental Margin, and Australia, *AAPG Bull.*, *73*, 1053-1064, 1989.

Brenner, A. C., C. J. Koblinsky, and B. D. Beckley, A preliminary estimate of geoid-induced variations in repeat orbit satellite altimeter observations, *J. Geophys. Res.*, *95*, 3033-3040, 1990.

Brooks, R. L., D. W. Lockwood, and H. D. W., Effects of islands in the Geosat footprint, *J. Geophys. Res.*, *95*, 2849-2855, 1990.

Calmant, S., J. Francheteau, and A. Cazenave, Elastic layer thickening with age of the oceanic lithosphere: a tool for prediction of the age of volcanoes or oceanic crust, *Geophys. J. Int.*, *100*, 59-67, 1990.

Calmant, S., and A. Cazenave, Anomalous elastic thickness of the oceanic lithosphere in the south-central Pacific, *Nature*, *328*, 236-238, 1987.

Cartwright, D. E., and R. D. Ray, Ocean tides from Geosat altimetry, *J. Geophys. Res.*, *95*, 3069-3090, 1990.

Cazenave, A., and K. Dominh, Global relationship between oceanic geoid and seafloor depth: New results, *Geophys. Res. Lett.*, *14*, 1-4, 1987.

Cazenave, A., K. Dominh, M. Rabinowicz, and G. Ceuleneer, Geoid and depth anomalies over ocean swells and troughs: Evidence of an increasing trend of the geoid to depth ratio with age of plate, *J. Geophys. Res.*, *93*, 8064-8077, 1988.

Cazenave, A., M. Monnereau, and D. Gilbert, Seasat gravity undulations in the central Indian Ocean, *Phys. Earth Planet. Inter.*, *48*, 130-141, 1987.

Cheney, R. E., B. C. Douglas, R. W. Agreen. L. L. Miller, D. L. Porter, and N. S. Doyle, Geosat altimeter geophysical data record user handbook, *NOAA Tech. Memo., NOS NGS-46*, 32 pp., 1987.

Cochran, J. R., Somali Basin, Chain Ridge, and origin of the Northern Somali Basin gravity and geoid low, *J. Geophys. Res.*, *93*, 11985-12008, 1988.

Coffin, M. F., and P. D. Rabinowitz, Reconstruction of Madagascar and Africa: evidence from the Davie fracture zone and western Somali Basin, *J. Geophys. Res.*, *92*, 9385-9406, 1987.

Craig, C. H., and D. T. Sandwell, Global distribution of seamounts from Seasat profiles, J. Geophys. Res., 93, 10408-10420, 1988.

Crough, S. T., Geoid anomalies across fracture zones, *Earth Planet. Sci. Lett.*, *44*, 224-230, 1979.

DeMets, C., R. G. Gordon, D. F. Argus, and S. Stein, Current plate motions, *Geophys. J. R. Astr. Soc.*, *101*, 425-478, 1990.

Denker, H., and R. H. Rapp, Geodetic and oceanographic results from the analysis of 1 year of Geosat data, *J. Geophys. Res.*, *95*, 13151-13168, 1990.

Douglas, B. C., and R. E. Cheney, Geosat - Beginning a new era in satellite oceanography, *J. Geophys. Res.*, *95*, 2833-2836, 1990.

Driscoll, M. L., and B. Parsons, Cooling of the oceanic lithosphere-evidence from geoid anomalies across the Udintsev and Eltanin fracture zones, *Earth Planet. Sci. Lett.*, *88*, 289-307, 1988.

Emery, W. J., G. H. Born, D. G. Baldwin, and C. L. Norris, Satellite-derived water vapor corrections for Geosat altimetry, *J. Geophys. Res.*, *95*, 2953-2964, 1990.

Fairhead, J. D., South East Asia gravity project. University of Leeds, Leeds, LS2 9JT, United Kingdom, 02, 1990.
Filmer, P. E., and M. K. McNutt, Geoid anomalies over the Canary-Islands group, *Mar. Geophys. Res., 11*, 77-87, 1989
Fleitout, L., C. Dalloubeix, and C. Moriceau, Small-wavelength geoid and topography anomalies in the South Atlantic Ocean - a clue to new hot-spot tracks and lithospheric deformation, *Geophys. Res. Lett., 16*, 637-640, 1989.
Freedman, A. P., and B. Parsons, Geoid anomalies over two South Atlantic Fracture Zones, *Earth Planet. Sci. Lett., 100*, 18-41, 1990.
Gahagan, L. M., C. R. Scotese, J. Y. Royer, D. T. Sandwell, J. K. Winn, R. L. Tomlins, M. I. Ross, J. S. Newman, R. D. Muller, C. L. Mayes, L. A. Lawver, and C. E. Heubeck, Tectonic fabric map of the ocean basins from satellite altimetry data, *Tectonophysics, 155*, 1-26, 1988.
Geos-3 Special Issue, The Geos-3 Project, *J. Geophys. Res., 84*, 3779-4079, 1979.
Gibert, D., C. Camerlynck, and V. Courtillot, Geoid anomalies across Ascension fracture zone and the cooling of the lithosphere, *Geophys. Res. Lett., 14*, 603-606, 1987.
Gibert, D., V. Courtillot, and J. L. Olivet, Seasat altimetry and the South Atlantic geoid 2. Short-wavelength undulations, *J. Geophys. Res., 94*, 5545-5559, 1989.
Goslin, J., and M. Diament, Mechanical and thermal isostatic response of the Del Cano Rise and Crozet Bank (southern Indian Ocean) from altimetry data, *Earth Planet. Sci. Lett., 84*, 285-294, 1987.
Haines, B. J., G. H. Born, G. W. Rosborough, J. G. Marsh, and others, Precise orbit computation for the Geosat exact repeat mission, *J. Geophys. Res., 95*, 2871-2885, 1990.
Hancock, D. W., R. L. Brooks, and D. W. Lockwood, Effects of height acceleration of Geosat heights, *J. Geophys. Res., 95*, 2843-2848, 1990.
Haxby, W. F., *Gravity Field of the World's Oceans*, National Geophysical Data Center, NOAA, Boulder, CO, 1987.
Haxby, W. F., and J. K. Weissel, Evidence for small-scale mantly convection from Seasat altimeter data, *J. Geophys. Res., 91*, 3507-3520, 1986.
Hayling, K., Satellite Gravity. PetroScan, Inc., S-411 04 Gothenburg, Sweeden, 1, 1990.
Hayne, G. S., and D. W. Hancock, Corections for the effects of significant wave height and attitude on Geosat radar altimeter measurements, *J. Geophys. Res., 95*, 2837-2842, 1990.
Hwang, C., High precision gravity anomaly and sea surface height estimation from Geos-3/Seasat satellite altimeter data, Dept. of Geodetic Science and Surveying, Rep. 399, The Ohio State University, 155 pp., 1989.
Jensen, J. J., and F. R. Wooldridge, The Navy Geosat mission: An introduction, *Johns Hopkins APL Technical Digest, 8*, 169, 1987.
Jung, W. Y., and P. D. Rabinowitz, Residual depth and residual geoid anomalies of the South Atlantic Ocean, *Mar. Geodesy, 13*, 33-52, 1989.
LeSchack, A. R., and R. V. Sailor, A preliminary model for Geosat altimeter data errors, *Geophys. Res. Lett., 15*, 1203-1206, 1988.
Liu, W. T., and D. Mock, The variability of atmospheric equivalent temperature for radar altimeter range correction, *J. Geophys. Res., 95*, 2933-2938, 1990.
Lonsdale, P., Geography and history of the Louisville hotspot chain in the southwest Pacific, *J. Geophys. Res., 93*, 3078-3104, 1988.
MacArthur, J. L., J. Marth P. C., and J. G. Wall, The Geosat radar altimeter, *Johns Hopkins APL Technical Digest, 8*, 176-181, 1987.
Maia, M., J. Diament, and M. Recq, Isostatic response of the lithosphere beneath the Mozambique ridge (SW Indian Ocean) and geodynamic implications, *Geophys. J. Int., 100*, 337-348, 1990.
Marks, K. M., and R. V. Sailor, Comparison of Geos-3 and Seasat altimeter resolution capabilities, *Geophys. Res. Lett., 13*, 697-700, 1986.
Marsh, J. G., A. C. Brenner, B. D. Beckley, and T. V. Martin, Global mean sea surface based upon Seasat altimeter data, *J. Geophys. Res., 91*, 3501-3506, 1986.
Marsh, J. G., C. J. Koblinsky, F. Lerch, S. M. Klosko, J. W. Robbins, R. G. Williamson, and G. B. Patel, Dynamic sea surface topography, gravity and improved orbit accuracies from the direct evaluation of Seasat altimeter data, *J. Geophys. Res., 95*, 13129-13150, 1990.
Marty, J. C., and A. Cazenave, Thermal evolution of the lithosphere beneath fracture zones inferred from geoid anomalies, *Geophys. Res. Lett., 15*, 593-596, 1988.
Marty, J. C., A. Cazenave, and B. Lago, Geoid anomalies across Pacific fracture zones, *Geophys. J., 93*, 1-23, 1988.
Mayes, C. L., L. A. Lawver, and D. T. Sandwell, Tectonic history and new isochron chart of the South Pacific, *J. Geophys. Res., 95*, 8543-8567, 1990.
McAdoo, D. C., Gravity field of the southeast Central Pacific from Geosat exact repeat mission data, *J. Geophys. Res., 95*, 3041-3047, 1990.
McAdoo, D. C., R. W. Agreen, R. E. Cheney, B. C. Douglas, N. S. Doyle, L. Miller, and E. L. Timmerman, Geosat/Geodeitc Mission geophysical data records: Format and contents, *NOAA Tech. Memo.*, 10 pp., 1990.
McAdoo, D. C., and D. T. Sandwell, On the source of cross-grain lineations in the Central Pacific gravity field, *J. Geophys. Res., 94*, 9341-9352, 1989.
McConathy, D. R., and C. C. Kilgus, The Navy Geosat mission: An overview, *Johns Hopkins APL Technical Digest, 8*, 170-175, 1987.
McNutt, M., Thermal and mechanical properties of the Cape Verde Rise, *J. Geophys. Res., 93*, 2784-2794, 1988.
McNutt, M. K., and A. V. Judge, The superswell and mantly dynamics beneath the South Pacific, *Science, 248*, 933-1048, 1990.
McNutt, M. K., and L. Shure, Estimating the compensation depth of the Hawaiian Swell with linear filters, *J. Geophys. Res., 91*, 13915-13923, 1986.
Mitchell, J. L., Z. R. Hallock, and J. D. Thompson, REX and Geosat: Progress in the first year, *Johns Hopkins APL Technical Digest, 8*, 234-244, 1987.
Monaldo, F., Path length variations caused by atmospheric water vapor and their effects on the measurement of mesoscale ocean circulation features by a radar altimeter, *J. Geophys. Res., 95*, 2923-2932, 1990.
Monnereau, M., and A. Cazenave, Depth and geoid anomalies over oceanic hotspot swells: A global survey, *J. Geophys. Res., 95*, 15429-15438, 1990.
Moriceau, C., and L. Fleitout, A directional analysis of the small wavelength geoid in the Pacific, *Geophys. Res. Lett., 16*, 251-254, 1989.
Musman, S., A. Drew, and B. Douglas, Ionospheric effects on Geosat altimeter observations, *J. Geophys. Res., 95*, 2965-2967, 1990.
Parmentier, E. M., and W. F. Haxby, Thermal stress in the oceanic lithosphere: Evidence from geoid anomalies at fracture zones, *J. Geophys. Res., 91*, 7193-7204, 1986.
Pavlis, J. K., and R. H. Rapp, The development of an isostatic gravitational model to degree 360 and its use in global gravity modelling, *Geophys. J. Int., 100*, 369-378, 1990.
Ping, C. S., Height errors introduced into the analysis of radar altimetry data by use of the simplified brown model, *Int. J. of Remote Sensing, 11*, 561-575, 1990.
Rapp, R. H., The decay of the spectrum of the gravitational potential and the topography of the Earth, *Geophys. J. Int., 99*, 449-455, 1989.
Royer, J. Y., P. Patriat, H. W. Bergh, and C. R. Scotese, Evolution of the southwest Indian Ridge from the late cretaceous (anomaly 34) to the middle Eocene (anomaly 20), *Tectonophysics, 155*, 235-260, 1988.
Royer, J. Y., and D. T. Sandwell, Evolution of the eastern Indian Ocean since the late cretaceous - constraints from Geosat altimetry, *J. Geophys. Res., 94*, 13,755-13,782, 1989.
Royer, J. Y., J. G. Sclater, and D. T. Sandwell, A preliminary tectonic fabric chart of the Indian Ocean, *Earth Planet. Sci., 98*, 7-24, 1989.
Sailor, R. V., and A. R. LeSchack, Preliminary determination of the Geosat radar altimeter noise spectrum, *Johns Hopkins APL Technical Digest, 8*, 182-183, 1987.
Sandwell, D. T., Thermomechanical evolution of oceanic fracture zones, *J. Geophys. Res. 89*, 11401-11413, 1984.
Sandwell, D. T., Biharmonic spline interpolation of Geos-3 and Seasat altimeter data, *Geophys. Res. Lett., 14*, 139-142, 1987.
Sandwell, D. T., and K. R. MacKenzie, Geoid height versus topography for oceanic plateaus and swells, *J. Geophys. Res., 94*, 7403-7418, 1989.
Sandwell, D. T., and D. C. McAdoo, Marine gravity of the Southern Ocean and Antarctic margin from Geosat, *J. Geophys. Res., 93*, 10389-10396, 1988.
Sandwell, D. T., and D. C. McAdoo, High-accuracy, high-resolution gravity profiles from 2 years of the Geosat exact repeat mission, *J. Geophys. Res., 95*, 3049-3060, 1990.
Sandwell, D. T., and M. L. Renkin, Compensation of swells and plateaus in the North Pacific: No direct evidence for mantle convection, *J. Geophys. Res., 93*, 2775-2783, 1988.
Seasat Special Issue I, Geophysical Evaluation, *J. Geophys. Res., 87*, 3173-3483, 1982.
Seasat Special Issue II, SCientific Results, *J. Geophys. Res., 88*, 1529-1952, 1983.
Shaw, P. R., Investigations of relative plate motions in the South Atlantic using Seasat altimeter data, *J. Geophys. Res., 92*, 9363-9375, 1987.
Shaw, P. R., An investigation of small-offset fracture zone geoid waveforms, *Geophys. Res. Lett., 15*, 192-195, 1988.
Shaw, P. R., and S. C. Cande, High-resolution inversion for South Atlantic plate kinematics using joint altimeter and magnetic anomaly data, *J. Geophys. Res., 95*, 2625-2644, 1990.
Sheehan, A. F., and M. K. McNutt, Constraints on thermal and mechanical structure of the ocean lithosphere at the Bermuda Rise from geoid height and depth anomalies, *Earth Planet. Sci. Lett., 93*, 377-391, 1989.
Shum, C. K., D. N. Yuan, J. C. Ries, J. C. Smith, and a. others, Precision orbit determination for the Geosat exact repeat mission, *J. Geophys. Res., 95*, 2887-2898, 1990.
Small, C., and D. T. Sandwell, An abrupt change in ridge axis gravity with spreading rate, *J. Geophys. Res., 94*, 17383-17392, 1989.
Smith III, S. L., G. B. West, and C. W. Malyevac, Determination of ocean geodetic data from Geosat, *Johns Hopkins APL Technical Digest, 8*, 197-200, 1987.
Stein, C. A., S. Cloetingh, and R. Wortel, Seasat-derived gravity constraints on stress and deformation in the northeastern Indian Ocean, *Geophys. Res. Lett., 16*, 823-826, 1989.
Stewart, R. H., *Methods of Satellite Oceanography*, Berkley, California: Univ. of Calif. Press, 1985.
Stock, J., and P. Molnar, Revised history of early Tertiary plate motion in the south-west Pacific, *Nature, 325*, 495-499, 1987.
Tapley, B. D., R. S. Nerem, C. K. Shum, J. C. Ries, and D. N. Yuan, Circulation from a joint gravity field solution determination of the general ocean, *Geophys. Res. Lett., 15*, 1109-1112, 1988.
Van Hee, D. H., Preliminary results from the processing of a limited set of Geosat radar altimeter data, *Johns Hopkins APL Technical Digest, 8*, 201-205, 1987.
Walsh, E. J., F. C. Jackson, E. A. Uliana, and R. N. Swift, Observations on electromagnetic bias in radar altimeter sea surface measurements, *J. Geophys. Res., 94*, 14575-14584, 1989.
Watts, A. B., On geoid heights derived from Geos-3 altimeter data and flexure of the lithosphere along the Hawaiian-Emperor seamount chain, *J. Geophys. Res., 84*, 3817-3826, 1979.
Watts, A. B., J. K. Weissel, R. A. Duncan, and R. L. Larson, Origin of the Louisville Ridge and its relationship to the Eltanin fracture zone system, *J. Geophys. Res., 93*, 3051-3077, 1988.
Wessel, P., and W. F. Haxby, Geoid anomalies at fracture zones and thermal models for the oceanic lithosphere, *Geophys. Res. Lett., 16*, 827-830, 1989.
Wessel, P., and W. F. Haxby, Thermal stresses, differential subsidence, and flexure at oceanic fracture zones, *J. Geophys. Res., 95*, 375-391, 1990.
Winterer, E. L., and D. T. Sandwell, Evidence from en-echelon cross-grain ridges for tensional cracks in the Pacific Plate, *Nature, 329*, 534-537, 1987.
Zimbelman, D. F., and A. J. Busalacchi, The wet tropospheric range correction - product intercomparisons and the simulated effect for tropical Pacific altimeter retrievals, *J. Geophys. Res., 95*, 2899-2922, 1990.
Zlotnicki, V., and J. G. Marsh, Altimetry, ship gravimetry, and the general circulation of the North Atlantic, *Geophys. Res., Lett., 16*, 1011-1014, 1989.

(Received November 2, 1990;
accepted February 1, 1991.)